

# Faraday waves in Bose–Einstein condensate: From instability to nonlinear dynamics

Kasumi Okazaki<sup>1</sup>, Junsik Han<sup>1</sup>, and Makoto Tsubota<sup>2</sup>

<sup>1</sup>*Department of Physics, Osaka City University, 3-3-138 Sugimoto, 558-8585 Osaka, Japan and*

<sup>2</sup>*Department of Physics & Nambu Yoichiro Institute of Theoretical and Experimental Physics (NITEP) & The OCU Advanced Research Institute for Natural Science and Technology (OCARINA), Osaka City University, 3-3-138 Sugimoto, Sumiyoshi-ku, Osaka 558-8585, Japan*

(Dated: December 7, 2020)

We numerically study the dynamics of Faraday waves in a cigar-shaped Bose–Einstein condensate (BEC) subject to periodic modulation of the interaction. After the modulation starts, Faraday waves appear and, thereafter, the BEC enters the “nonlinear regime”, in which several collective modes are excited. By maintaining the modulation without dissipation, the kinetic energy that contributes to the density gradient causes quasiperiodic motion and increases monotonically. In the nonlinear regime, the dips in the density similar to dark solitons move around in the BEC, intersecting with each other and maintaining their shapes. On the other hand, even by turning off the modulation, Faraday waves and the nonlinear regime appear. The kinetic energy converges to the statistical steady state. The calculation of the modulation with the dissipation illustrates the collapse and revival of Faraday waves. When the dissipation is small, the appearance and collapse of the Faraday waves and the nonlinear regime occur again.

## I. INTRODUCTION

Fluid mechanics has been studied in various fields of research such as turbulence [1], vortices [2, 3], hydrodynamic instability [4], and pattern formations [5]. In pattern formation, as the control parameters increase, complex bifurcation and various nonequilibrium phenomena appear through nonlinear interaction. Spatial pattern formation in a classical fluid is primarily categorized into three types: Taylor–Couette flow, Rayleigh–Benard convection, and parametric surface waves. The representative example of the parametric surface waves is Faraday waves [6], which are regular standing waves that appear on the surface of a vibrating fluid. These waves are excited with twice of a natural frequency. In 1831, Faraday waves were observed in an experiment conducted by vertically modulating a container containing fluids. These dynamics are governed by an equation of pattern formations known as the Mathieu equation [7]:

$$\frac{d^2x}{dt^2} + \Omega^2 [1 + \epsilon \cos(\omega t)] x = 0, \quad (1)$$

where  $x$  represents the fluctuation from a stationary state,  $\epsilon$  is the drive amplitude,  $\Omega$  is the natural frequency, and  $\omega$  is the drive frequency. When the higher order of the fluctuations of surface waves can be ignored, the Euler equation reduces to a Mathieu equation [7]. The Floquet analysis of a Mathieu equation yields an infinite series of resonances at  $\omega = 2\Omega/n$  for integer  $n$ , and the first ( $n = 1$ ) resonance excites Faraday waves. Several studies on Faraday waves have demonstrated solitons [8], pattern formations [9–11], and space and time modulation [11–13].

The quantum hydrodynamics of a Bose–Einstein condensate (BEC) [14] have also been studied for topics such as quantum turbulence [15], quantized vortices, quantum hydrodynamic instability, and pattern formations. The dynamics of a BEC with a wave function  $\psi$  are governed

by the Gross–Pitaevskii (GP) equation [16] as follows:

$$(i - \gamma)\hbar \frac{\partial \psi}{\partial t} = -\frac{\hbar^2}{2m} \Delta \psi + V\psi + g|\psi|^2\psi, \quad (2)$$

where  $m$  is the mass of an atom,  $V$  is the potential, and  $g$  represents the interaction of atoms. We introduce the term  $\gamma$  to describe the dissipation [17, 18]. Faraday waves in a BEC are excited experimentally by modulation of the trapping potential [19] or the interaction [20]. When  $V = 0$ , substituting  $\psi = \exp[-i\frac{\alpha}{\omega} \sin(2\omega t)] [1 + w(t) \cos(kx)]$  in the GP equation (Eq. (2)) by modulating the interaction gives the Mathieu equation [21]. If a BEC is trapped by a cigar-shaped potential, forceful resonant waves similar to Faraday waves are experimentally excited with  $\omega = 2\omega_r$  along the longitudinal direction by the modulation of the potential along the tight direction or the modulation of the interaction [19, 20]. These parametrically driven excited waves have been studied theoretically [22, 23]. Although these situations in a BEC are different from the original Faraday waves in a classical fluid, such excited waves in a BEC can be considered as an analog to Faraday waves.

The Faraday waves of a BEC have been studied theoretically and experimentally. Previous studies [19, 20] have reported that Faraday waves appear by modulating the trapping potential or the interaction. In the first case of modulating the trapping potential [19], the experiments were conducted by periodic modulation of the transverse trapping frequencies of a cigar-shaped BEC. Engels *et al.* observed the appearance of longitudinal Faraday waves with  $\omega = 2\omega_r$ , where the trapping frequency  $\omega_r$  corresponds to  $\Omega$  (Eq. (1)). They also determined the instability of Faraday waves by strongly driving the transverse breathing mode. In the second case, when the interaction is modulated in a cigar-shaped BEC [20], Nguyen *et al.* observed Faraday waves after the modulation time of  $t_m = 5$  ms, followed by a holding time of  $t_h = 20$  ms. There have also been certain theoretical and

numerical studies of Faraday waves [22–27]. When  $V = 0$  [24], Staliunas *et al.* solved the GP equation by modulating the interaction. The results indicated the evolutions of patterns and resonance tongues of parametric instability for conservative and dissipative systems. They [25] also indicated the appearance of a self-parametric instability in the case of one-dimensional cigar-shaped and two-dimensional disk-shaped BECs. Furthermore, the study represents the dependency of the numerically determined threshold on the modulation frequency. Balaz *et al.* [23] numerically calculated the time evolutions of the radially integrated longitudinal density profile by modulating the trapping potential in a collisionally inhomogeneous BEC. The time evolutions indicated that the appearance of Faraday waves is accompanied by the excitation of the collective modes, and these waves are set in the forcefully destabilized condensate. Faraday waves have been studied in two-component BECs [26] by Balaz *et al.*. When the trapping potential is modulated, the time evolutions from two initial states of dark-bright symbiotic pair states and segregated states were simulated by coupled GP equations. As the result, Faraday waves were excited simultaneously in the two components.

In this study, we examine Faraday waves, instability, and nonlinear regime by modulating the interaction in a cigar-shaped BEC. We assume that the grand-state hyperfine level  $|F = 1, m_F = 1\rangle$  of the  ${}^7\text{Li}$  atom and the s-wave scattering length of the atoms is controlled by Feshbach resonance. We carry out three types of calculations. One is by maintaining the modulation, the other is by turning the modulation off at  $t_m = 5$  ms without the dissipation  $\gamma$ , and the third one is maintaining the modulation along with the dissipation  $\gamma$ . We numerically illustrate the appearance of Faraday waves in all the calculations for  $\omega = 2\omega_r$ . These waves appear for the modulation amplitude  $1 \text{ G} < \Delta B < 9 \text{ G}$ . Thereafter, the system enters the nonlinear regime when the energies between the injection and the dissipation are not balanced. This regime consists of the excitations of the collective modes and represents the periodic motion of the density dips. The collapse and revival of Faraday waves occur only with the dissipation.

This paper is organized as follows. In Sec. II, we describe our numerical scheme of a two-dimensional GP equation and the conditions of our calculations. In Sec. III, we present our numerical results that indicate that Faraday waves and the instability. Thereafter, the BEC without the dissipation enters the nonlinear regime. The nonlinear regime discussed in Sec. IV consists of the excitations of collective modes, and Faraday waves in the BEC with the dissipation repeats the expansion and collapse when the interaction is maintained to apply the modulation. Finally, in Sec. V, we summarize the study.

## II. CALCULATION

We numerically solve the two-dimensional GP equation (Eq. (2)) by modulating the interaction parameter using the spectral method. Following the previous research [20], we consider a cigar-shaped BEC of  $8 \times 10^5$   ${}^7\text{Li}$  atoms in a harmonic trap,  $V = \frac{1}{2}m(z^2\omega_z^2 + r^2\omega_r^2)$ . The axial and radial trapping frequencies are  $\omega_z = 2\pi \times 8$  Hz and  $\omega_r = 2\pi \times 512$  Hz. The spatial mesh sizes in the  $r$  and  $z$  directions are  $dr = 0.025$  and  $dz = 0.025$ , respectively. The interaction parameter is modulated using Feshbach resonance [28]. The s-wave scattering length is controlled by the magnetic field [16]; thus, the interaction parameter can be expressed as follows:

$$g = \frac{\hbar^2}{m} a_{bg} \left( 1 + \frac{\Delta}{B(t) - B_\infty} \right), \quad (3)$$

where  $a_{bg} = -24.5a_0$ ,  $a_0$  is the Bohr radius,  $\Delta = 192.3$  G, and  $B_\infty = 736.8$  G. The oscillation of the magnetic field is expressed as follows:

$$B(t) = \bar{B} + \Delta B \sin(\omega t), \quad (4)$$

where  $\bar{B} = 577.4$  G is the mean magnetic field,  $\Delta B$  is the amplitude, and  $\omega$  is the modulation frequency. To investigate the amplitudes  $\Delta B$  and the modulation frequencies  $\omega$  necessary for the appearance of Faraday waves, we calculate the GP equation using the various values of  $\Delta B$  and  $\omega$ . These frequencies correspond to the modes  $n$  of the Mathieu equation (Eq. (1)). It is convenient to introduce dimensionless variables here:

$$t = \frac{1}{\omega_z} \tilde{t}, z = a_z \tilde{z}, \psi = \sqrt{N} \frac{\tilde{\psi}}{a_z}, \quad (5)$$

where  $a_z = \sqrt{\frac{\hbar}{m\omega_z}}$  is the length along the  $z$ -axis and  $N$  is the total particle number expressed as follows:

$$N = \int \int |\psi(r, z)|^2 dr dz. \quad (6)$$

The GP equation (Eq. (2)) is reduced to a dimensionless form:

$$(i - \gamma) \frac{\partial \tilde{\psi}}{\partial \tilde{t}} = -\frac{1}{2} \Delta \tilde{\psi} + \tilde{V} \tilde{\psi} + \tilde{g} |\tilde{\psi}|^2 \tilde{\psi}. \quad (7)$$

The dimensionless potential and interaction take the following forms:  $\tilde{V} = \frac{1}{2} \left( \tilde{z}^2 + \tilde{r}^2 \frac{\omega_r^2}{\omega_z^2} \right)$  and

$$\tilde{g} = 2\sqrt{2\pi} N \frac{a_{bg}}{a_r} \left( 1 + \frac{\Delta}{B(t) - B_\infty} \right), \quad (8)$$

where  $a_r = \sqrt{\frac{\hbar}{m\omega_r}}$  is the length along the  $r$ -axis. The dimensionless symbol tilde is omitted below for simplicity.

To evaluate how Faraday waves appear depending on the modulation time  $t_m$  and the dissipation, we calculate

the GP equation for three cases. For  $\gamma = 0$ , the first case is to maintain the modulation and the second is turning the modulation off at  $t_m = 5$  ms. The third case is to maintain the modulation along with the dissipation  $\gamma$ . We calculate the third case because a system with dissipation is realistic and demonstrates a qualitatively different dynamics than one without dissipation.

Next, we calculate the kinetic energy. The total energy  $E_{tot}$  of a BEC is expressed as follows:

$$E_{tot} = \int \left[ \frac{1}{2} |\nabla\psi|^2 + V|\psi|^2 + g|\psi|^4 \right] dr, \quad (9)$$

where the first, second, and third terms on the right-hand side are the kinetic, potential, and interaction energies, respectively. For a wave function expressed as  $\psi = |\psi|e^{i\theta}$ , the kinetic energy is calculated as follows:

$$|\nabla\psi|^2 = |\nabla|\psi||^2 + |\psi|^2 (\nabla\theta)^2, \quad (10)$$

where the first and second terms represent the contributions of the density gradient and the superfluid velocity  $v_s = \frac{\hbar}{m} (\nabla\theta)$  to the kinetic energy.

### III. EXCITATION AND DYNAMICS OF FARADAY WAVES

In this section, we present the results of the three cases mentioned above. We also discuss the instability against the modulation and excitation of Faraday waves. We discuss two main results in this section. First, the calculations for  $\omega = 2\omega_r$  and  $1 \text{ G} < \Delta B < 9 \text{ G}$  indicate the appearance of Faraday waves. The onset time of the appearance is hundreds of milliseconds after the modulation started. The second result is that the dynamics changes to the nonlinear regime, such as excitations of collective modes similar to wave turbulence after the excitation of Faraday modes in the dissipationless case. However, the calculation along with the dissipation indicates that Faraday waves appear and collapse with a cycle of hundreds of milliseconds without entering the nonlinear regime. The analysis of the nonlinear regime is described in Sec. IV, and this section describes only the results of Faraday waves and instability.

#### A. Appearance of Faraday waves without dissipation ( $\gamma = 0$ )

When we continue to apply the modulation without dissipation, Faraday waves that have regularly spaced patterns are excited after  $t \simeq 68$  ms. Figure 1 displays the typical dynamics of the Faraday wave density. These waves are excited at  $t = 71.32$  ms and start to collapse at  $t = 71.52$  ms. After the suppression, the excited waves reappear at  $t = 72.32$  ms. This collapse and revival for a few milliseconds are repeated. Faraday waves are characterized by the single dominant peak of a fast Fourier

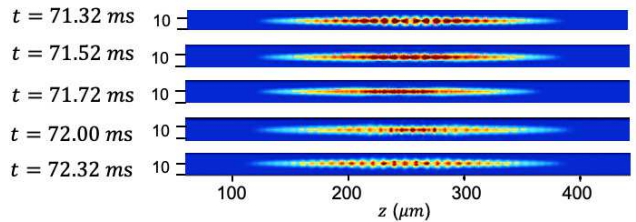


FIG. 1: Dynamics of Faraday waves during  $t = 71.32 - 72.32$  ms in BEC. These figures represent density images of Faraday waves in harmonic trap. Driving frequency  $\omega = 1024 \times 2\pi$  Hz and amplitude  $\Delta B = 5$  G. This calculation maintains modulation without  $\gamma$ .

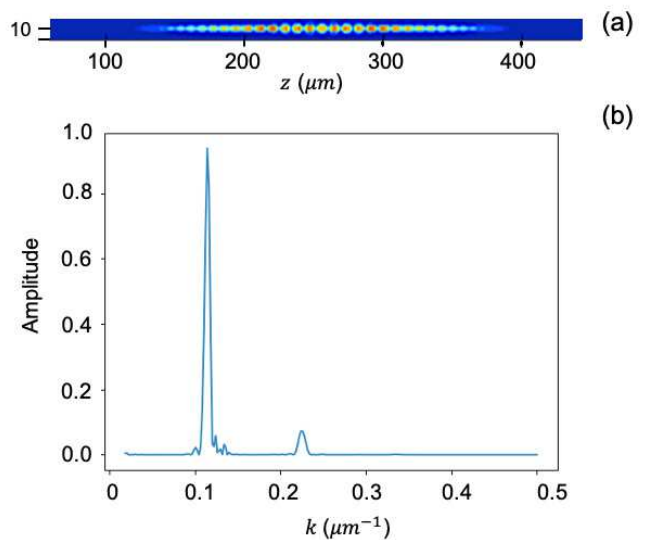


FIG. 2: Appearance of Faraday waves at  $t \simeq 80$  ms. Driving frequency  $\omega = 1024 \times 2\pi$  Hz and amplitude  $\Delta B = 5$  G. This calculation maintains modulation without  $\gamma$ . (a) Density image of Faraday waves and (b) FFT of one-dimensional density.

transform (FFT). The spectrum is calculated by integrating  $|\psi|^2$  along the  $r$ -axis:

$$|\psi_{1D}(z, t)|^2 = \int_0^\infty 2\pi r |\psi(r, z, t)|^2 dr. \quad (11)$$

We apply the FFT to the one-dimensional density  $|\psi_{1D}|^2$  and obtain the spectrum of regularly spaced patterns. A typical image of Faraday patterns is displayed in Fig. 2. Figures 2 (a) and (b) display the density and FFT spectrum, respectively, when these waves appear. Figure 2 (b) indicates that the spectrum is characterized by a single peak  $k \simeq 0.12 \mu\text{m}^{-1}$  corresponding to a spatial period of the density  $\lambda \simeq 8.70 \mu\text{m}$ . This result is similar to the experimental result [20]. The beginning of the animation [29, 30] represents the time development of Faraday waves.

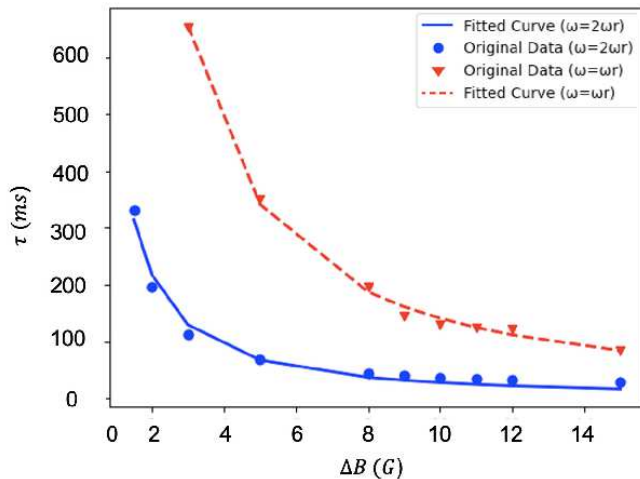


FIG. 3: Instability onset times  $\tau$  plotted as a function of  $\Delta B$ . Blue circles and red triangles represent results of calculations with modulation for  $\omega = 2\omega_r$  and  $\omega = \omega_r$  without  $\gamma$ , respectively. Blue solid and red dashed lines are fitted curves.

We also observe that the instability onset time  $\tau$  depends on  $\omega$  and  $\Delta B$ . The instability onset time  $\tau$  refers to the time at which the excited density waves such as Faraday modes and other modes appear for the first time. The onset time for Faraday waves decreases with  $\Delta B$ , as depicted in Fig. 3, and has different values for each  $\omega$ . That is, the instability appears quickly as the injected energy depending on  $\Delta B$  increases. When  $\omega = \frac{2}{n}\omega_r$  ( $1 < n$ ), the density waves of mode  $n$  appear. This onset time is generally delayed compared to that of the Faraday waves and this resonance is the strongest.

Figure 4 illustrates the appearance of the various density waves and the nonlinear regime depending on  $\omega$  and  $\Delta B$ . Faraday waves are not clearly observed even at  $\omega = 2\omega_r$  for the modulation amplitude of  $\Delta B \leq 1$  G or  $\Delta B \geq 9$  G. For  $\Delta B \geq 9$  G, Faraday modes appear along with other collective modes; however, it quickly casts the system into the nonlinear regime. When  $\Delta B \leq 1$  G, the system is almost stationary because the modulation amplitude is too small. Hence, Faraday waves clearly appear for  $1 \text{ G} < \Delta B < 9 \text{ G}$ . However, if the modulation frequency  $\omega$  and amplitude  $\Delta B$  are too small, these waves are not observed. Thus, in subsequent calculations, we primarily assume the conditions of  $\omega = 2\omega_r$  and  $\Delta B = 5$  G.

When we turn off the modulation at  $t_m = 5$  ms, Faraday waves appear at  $t \simeq 168$  ms and remain for 18.0 ms. The FFT is characterized by a single peak that corresponds to the spatial period  $\lambda \simeq 10 \mu\text{m}$ , similar to the first calculation of maintaining the modulation depicted in Fig. 2. It is essential to note that Faraday waves appear a short time after turning off the modulation at  $t_m = 5$  ms, and the onset time of 168 ms is delayed compared to that of the first calculation of the modula-

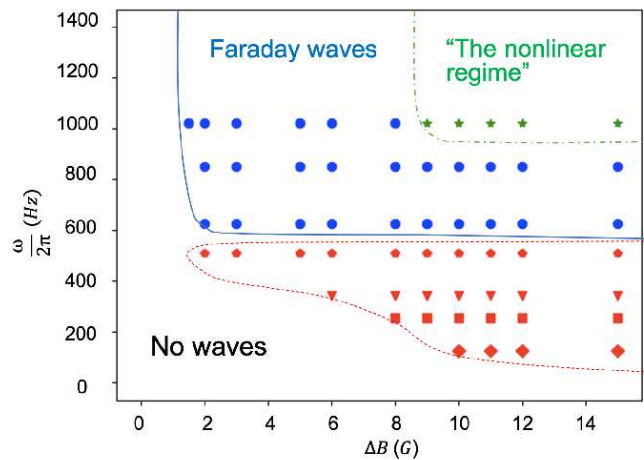


FIG. 4: Phase diagram of instability for  $\omega$  and  $\Delta B$ . We calculate GP equation for  $\omega = 2\omega_r$  ( $n = 1$ ),  $\omega = \frac{5}{3}\omega_r$  ( $n = \frac{6}{5}$ ),  $\omega = \frac{3}{2}\omega_r$  ( $n = \frac{4}{3}$ ),  $\omega = \omega_r$  ( $n = 2$ ),  $\omega = \frac{2}{3}\omega_r$  ( $n = 3$ ),  $\omega = \frac{1}{2}\omega_r$  ( $n = 4$ ), and  $\omega = \frac{1}{4}\omega_r$  ( $n = 8$ ) by maintaining modulation without  $\gamma$ . Trapping frequency  $\omega_r = 2\pi \times 512$  Hz. Blue circles and red pentagons represent appearance of Faraday modes ( $n = 1$ ) and resonance modes ( $n = 2$ ), respectively. Red triangles, red squares, red diamonds, and green stars represent modes  $n = 3$ ,  $n = 4$ , and  $n = 8$  and nonlinear regime, respectively. Regions surrounded by solid blue line, dashed green line, and dotted red line represent excitation of Faraday waves, nonlinear regime, and density waves of modes of  $n \neq 1$ , respectively. Other region depicts no waves.

tion. This implies that the BEC retains the memory of the modulation even after it is turned off, and Faraday waves appear at  $t \simeq 168$  ms.

#### B. Appearance of Faraday waves with dissipation ( $\gamma \neq 0$ )

The dynamics with  $\gamma$  yields significantly different results compared to that without  $\gamma$ . When the BEC is subject to continuous modulation and dissipation with  $\gamma = 0.03$ , the Faraday modes are excited at  $t \simeq 360$  ms. These waves remain for 24.8 ms. The density image and FFT spectrum are illustrated in Fig. 5. The FFT is characterized by only one peak, which corresponds to the spatial period  $\lambda \simeq 8.08 \mu\text{m}$ . Figure 5 depicts similar density distribution and FFT spectrum as for the first calculation without  $\gamma$ , depicted in Fig. 2. The significant difference is found in the dynamics after the appearance of Faraday waves, which will be discussed in detail in the following section.

#### IV. EXCITATION OF NONLINEAR REGIME

In this section, we consider the nonlinear regime, which consists of several collective modes. As described in the

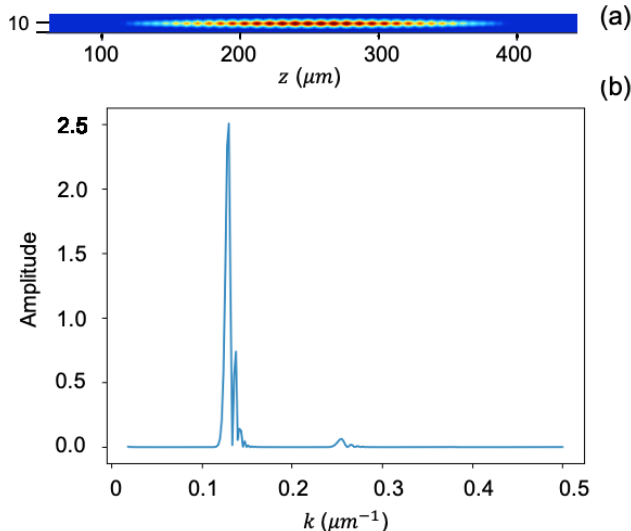


FIG. 5: Appearance of Faraday waves at  $t \simeq 372$  ms with dissipation  $\gamma = 0.03$ . Driving frequency  $\omega = 1024 \times 2\pi$  Hz and driving amplitude  $\Delta B = 5$  G. (a) Density image of Faraday waves and (b) FFT of one-dimensional density. These waves are characterized by single peak, similar to that in Fig. 2.

preceding section, there are two patterns for the appearance of the nonlinear regime. First, Faraday waves are excited initially, followed by other modes; eventually, the nonlinear regime appears. The other is caused when the injected energy is too strong; this regime appears suddenly, exciting several modes including the Faraday modes. In this section, we focus on the first case in which Faraday waves are followed by the appearance of the nonlinear regime. Interestingly, the dynamics for  $\gamma \neq 0$  are completely different from that for  $\gamma = 0$ . For  $\gamma \neq 0$ , Faraday waves continue to appear and disappear. This can be observed from the oscillation of the kinetic energy, consisting of the contributions of the density gradient and the superfluid velocity.

#### A. Dynamics of nonlinear regime without dissipation ( $\gamma = 0$ )

In the calculation for the modulation without  $\gamma$ , the nonlinear regime appears at  $t \simeq 88$  ms after the appearance of the Faraday waves. Figure 6 (a) presents the density image of the nonlinear regime, where the BEC cloud expands more along the  $z$ -axis than that depicted in Fig. 2 (a) at  $t \simeq 80$  ms. Figure 6 (b) depicts the appearances of multiple small peaks. These peaks correspond to the excitation of other collective modes as well as the Faraday modes. The animation presented in [29, 30] illustrates the time development of the density and FFT from the Faraday waves depicted in Fig. 2 to the nonlinear regime depicted in Fig. 6.

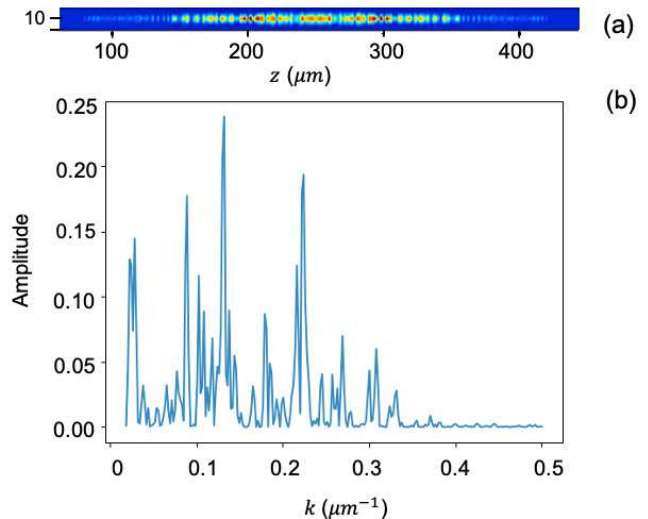


FIG. 6: Appearance of nonlinear regime for modulation at  $t \simeq 100$  ms without  $\gamma$ . Driving frequency  $\omega = 1024 \times 2\pi$  Hz and driving amplitude  $\Delta B = 5$  G. (a) Density image and (b) FFT of one-dimensional density of nonlinear regime.

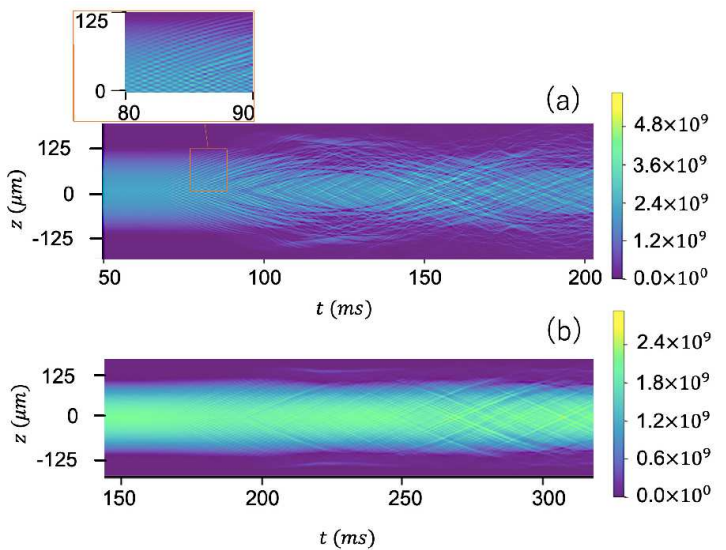


FIG. 7: Time evolution of density at  $\Delta B = 5$  G and  $\omega = 2\omega_r$ . Time evolution of density: (a) when modulation is continuously applied and (b) when modulation is turned off at  $t_m = 5$  ms without  $\gamma$ . Inset depicts appearance of Faraday waves.

Figure 7 presents the time evolutions of the density  $|\psi|^2$ . For maintaining the modulation (Fig. 7 (a)), several dips of the density move beyond the Thomas–Fermi radius ( $\sim 115\mu\text{m}$ ) and are reflected by the trapping potential. After that, the reflected dips return to the center of the BEC, move towards the opposite side, and are reflected again. These movements have a periodicity of about 240 ms. These dips intersect with each other

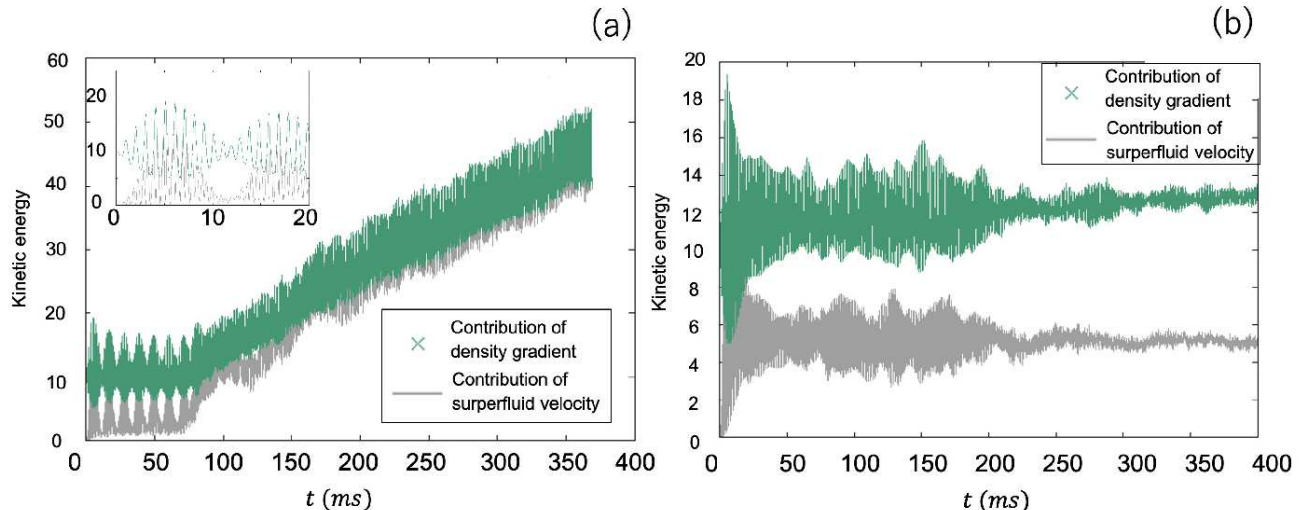


FIG. 8: Kinetic energy dividing contributions to density gradient and superfluid velocity as depicted in Eq. (10). Driving frequency  $\omega = 1024 \times 2\pi$  Hz and amplitude  $\Delta B = 5$  G. Green and gray plots represent the energy contributing to density gradient and superfluid velocity, respectively. Kinetic energy is calculated (a) for maintaining the modulation and (b) by turning the modulation off at  $t_m = 5$  ms without  $\gamma$ .

while maintaining their shapes. This behavior is similar to that of dark solitons. In the following section, we calculate the time evolution of a dark soliton and confirm that these dips are not dark solitons. A similar behavior was reported in a previous study [23], which addressed weakly inhomogeneous collisions and modulated the trapping potential. Figure 5 of [23] depicts the expansion and shrinking of density dips. Thus, the nonlinear regime is not unique to the interaction modulation of our case. Next, we depict the time evolution of the density in Fig. 7 (b) when the modulation is turned off at  $t_m = 5$  ms. The nonlinear regime appears at  $t \simeq 168$  ms; however, the expansion of the BEC is not clearly observed. This regime does not necessarily accompany the expansion and collapse of the system, as seen when the modulation is maintained.

To investigate the difference between the first and second calculations, we calculate the kinetic energy by dividing it into contributions (Eq. (10)) of the density gradient and the superfluid velocity, as depicted in Fig. 8. The fast oscillations of the kinetic energy with a period of about 1 ms correspond to the modulation of the interaction. Figure 8 (a) represents the kinetic energy while the modulation is maintained, and this energy causes quasiperiodic oscillations with periods of about 10 and 1 ms. Faraday waves appear at  $t \simeq 68$  ms, and the energy starts to increase at  $t \simeq 75$  ms. Thereafter, at  $t \simeq 88$  ms, the BEC enters the nonlinear regime. The total energy continues to increase because of the modulation. On the other hand, Fig. 8 (b) indicates that the kinetic energy becomes statistically steady after turning off the modulation. The kinetic energy causes quasiperiodic oscilla-

tions in this case too. Faraday waves appear at  $t = 168$  ms, and the amplitude of the oscillations of the kinetic energy is reduced after  $t \simeq 210$  ms. The behaviors in the first and second cases are significantly different; however, what happens is unclear, including the memory effect that causes the Faraday waves to appear a short time after the modulation is turned off.

Figure 7 (a) illustrates that several dips of density move around in the BECs and induce the nonlinear regime. To study whether the nonlinear regime is characterized by dark solitons, we compare the dip of the density with that of a dark soliton [16]. When the dark solitons have a density  $n_0$  in a stationary state and the minimum density value  $n_{min}$ , their velocity  $u$  is expressed as follows:

$$u = s \sqrt{\frac{n_{min}}{n_0}}, \quad (12)$$

with the sound velocity  $s = \sqrt{\frac{n_0 g}{m}}$ . The following phase difference exists across the dark solitons:

$$\Delta\phi = -2 \cos^{-1} \left( \frac{u}{s} \right). \quad (13)$$

The ratio  $n_{min}/n_0$  is approximately 0.001 and  $s = 340$   $\mu\text{m}/\text{ms}$  for the dips in our simulation. If the dips are dark solitons, the soliton velocity should be approximately 11  $\mu\text{m}/\text{ms}$ ; however, this velocity is larger than approximately 2  $\mu\text{m}/\text{ms}$  for the dips depicted in Fig. 7 (a). Dark solitons are expected to reflect a phase difference of approximately  $-\pi$ , which is not observed for the dips in our simulation. Therefore, we conclude that these dips do not represent dark solitons.

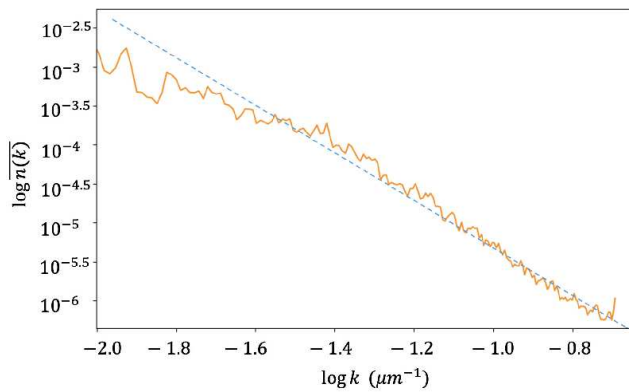


FIG. 9: Time-averaged spectrum  $\overline{n(k)}$ . Driving frequency  $\omega = 2\omega_r$  and amplitude  $\Delta B = 5$  G. This calculation is performed by maintaining the modulation without  $\gamma$ . Orange solid line represents time-averaged  $\overline{n(k)}$  for  $t \simeq 96.0 \sim 165.2$  ms. Blue dashed line represents fitting function  $\overline{n(k)} \propto k^{-3.09}$ .

Next, we calculate the spectrum  $n(k) = |\psi_k|^2$  for the nonlinear regime. Here, the time-averaged  $\overline{n(k)}$  is obtained for the half-period of the dips  $t \simeq 96.0 \sim 165.2$  ms, as depicted in Fig. 7 (a). Figure 9 illustrates the power law  $\overline{n(k)} \propto k^{-3.09}$ . The exponent  $-3.09$  is similar to the power  $-3.5$  of the typical wave turbulence [31, 32]. The spectrum  $\overline{n(k)}$  deviates from the power law at low wave numbers owing to the finite size effect. The system size corresponds to  $\log k = -2.2$ . The detailed studies of the turbulence and the exponent are beyond the scope of this paper.

### B. Dynamics of nonlinear regime with dissipation ( $\gamma \neq 0$ )

The calculations without  $\gamma$  indicate that the BEC enters the nonlinear regime after the appearance of Faraday waves. However, the calculation with  $\gamma = 0.03$  indicates that Faraday waves repeat the suppression and growth. The time development of these dynamics is presented in Fig. 10 (a). As illustrated, Faraday modes are excited at  $t \simeq 360$  ms, and they disappear at  $t \simeq 385$  ms. The BEC is stationary during the disappearance of these waves. Thereafter, the waves reappear at  $t \simeq 456$  ms and disappear at  $t \simeq 492$  ms. Subsequently, the suppression and growth of these waves are repeated several times with approximately the same period. Similar revival and collapse phenomena have also been reported experimentally [20]. Our simulations demonstrate that dissipation is indispensable for such phenomena. On the other hand, the result obtained for  $\gamma = 0.01$  indicates a significantly different behavior. Faraday waves appear at  $t \simeq 85$  ms, and the nonlinear regime appears at  $t \simeq 125$  ms. Interestingly, Faraday waves and the nonlinear regime repeat

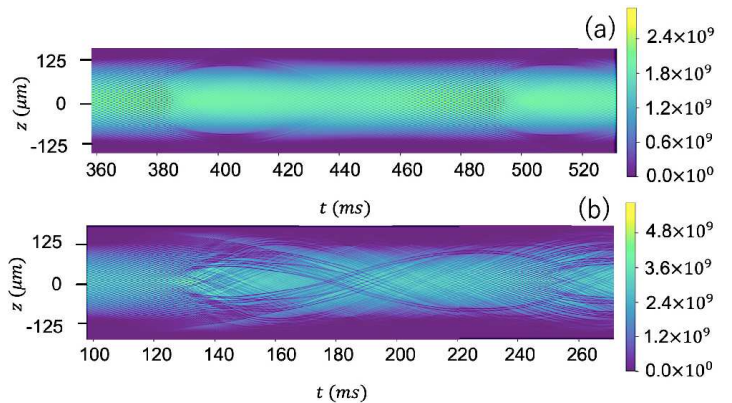


FIG. 10: Time evolution of density at  $\Delta B = 5$  G and  $\omega = 1024 \times 2\pi$  when modulations with (a)  $\gamma = 0.03$  and (b)  $\gamma = 0.01$  are maintained

the revival and collapse, as depicted in Fig. 10 (b). That is, Faraday waves and the nonlinear regime reappear at  $t \simeq 230$  ms and  $t \simeq 250$  ms, respectively. It should be noted that the reappearance of Faraday waves is accompanied by weak excitations of collective modes owing to the depression of the nonlinear regime.

To clarify the difference in the dynamics with and without  $\gamma$ , we show the time development of the kinetic energy. Figure 11 (a), for  $\gamma = 0.03$ , indicates that the kinetic energy owing to the density gradient starts to increase at  $t \simeq 320$  ms and decrease at  $t \simeq 360$  ms; thereafter, Faraday waves appear. At  $t \simeq 460$  ms, this energy increases again. In this case, the dynamics does not lead to quasiperiodic oscillations as depicted in Fig. 8 (a), and the kinetic energy is smaller than that in the case without  $\gamma$ . A comparison between Figs. 10 (a) and 11 (a) indicates that the oscillations of the kinetic energy correspond to the appearance and disappearance of Faraday waves, which is caused by the balance between the energy of injection and dissipation. Figure 11 (b), for  $\gamma = 0.01$ , indicates that the kinetic energy increases because  $\gamma$  is smaller than that depicted in Fig. 11 (a). The dynamics for  $\gamma = 0.03$  and  $\gamma = 0.01$  are completely different; however, their injection and dissipation energies are balanced in both cases.

When  $\gamma = 0.03$  and  $\Delta B = 15$  G, significantly more energy is injected into the BEC, and the nonlinear regime appears at  $t \simeq 39.8$  ms without Faraday waves. In this case, we cannot observe the suppression and growth of Faraday waves (similar to the nondissipative cases) because the injected energy is very large, implying that the balance between the injection and dissipation energies cannot be maintained.

The calculation with  $\gamma = 0.03$  is different from the nondissipative cases in three ways. First, the dissipation suppresses the excitations of the collective modes. At this time, the Faraday modes are also suppressed; however, they appear because they are most strongly excited

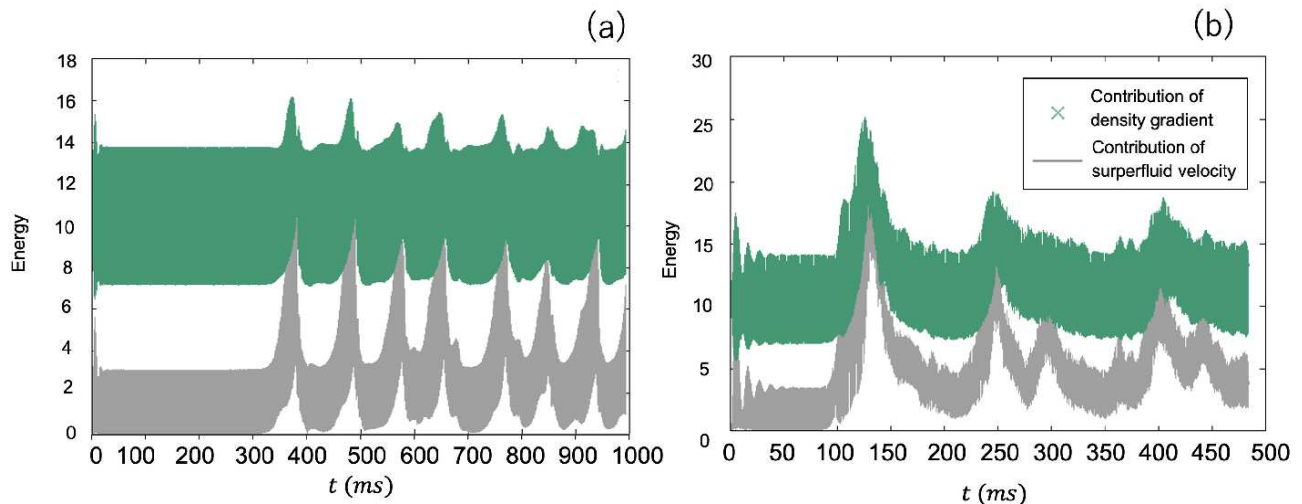


FIG. 11: Kinetic energy dividing contributions to density gradient and superfluid velocity as depicted in Eq. (10). Driving frequency  $\omega = 1024 \times 2\pi$  Hz and amplitude  $\Delta B = 5$  G. Green and gray plots represent energy contributing to density gradient and superfluid velocity, respectively. Kinetic energy is calculated by maintaining modulation with (a)  $\gamma = 0.03$  and (b)  $\gamma = 0.01$ .

against the dissipation, as depicted in Figs. 5 (b) and 10 (a). That is, the dissipation prevents the appearance of the nonlinear regime but not the revival of the Faraday waves. Second, the onset time of the Faraday waves with  $\gamma$  is delayed compared to that without  $\gamma$ . This is because the injected energy is swept away by the dissipation, and it takes more time to excite Faraday waves. Finally, the peak of the FFT for  $\gamma = 0.03$  is higher than that for  $\gamma = 0$ , implying that Faraday waves are more clearly observed for  $\gamma = 0.03$  than for  $\gamma = 0$ . The reason for this phenomenon is unknown.

### C. Dynamics of Faraday waves and nonlinear regime

In this section, we summarize the dynamics of Faraday waves and the nonlinear regime. The summary is presented in Table I. When we maintain the modulation without  $\gamma$ , the density of the BEC expands and shrinks continuously while maintaining the cigar-shape as that before the appearance of the Faraday waves. During this time, the kinetic energy produces a quasiperiodic motion, as depicted in Fig. 8 (a). After tens of milliseconds, the kinetic energy owing to the density gradient increases and the Faraday modes are excited, as depicted in Fig. 2. During the excitation of these modes, the collapse and revival of the Faraday waves are repeated with a period of a few milliseconds, as presented in Fig. 1. Next, these waves collapse completely and the condensate expands beyond the Thomas–Fermi radius, as depicted in Fig. 7 (a). Thereafter, the potential energy increases, as does the total energy. Therefore, other collective modes are excited and the dynamics enters the nonlinear regime, which accompanies the expansion and collapse of the

BEC. If we continue the excitation, the BEC may eventually collapse and the system goes beyond what the GP mean-field can describe. On the other hand, the calculation upon turning off the modulation at  $t_m = 5$  ms without  $\gamma$  indicates the appearance of Faraday waves and the nonlinear regime similar to Fig. 7 (b). There are three differences associated: the first is the onset time of the instability. The onset time when the excitation is turned off is delayed as compared with that when the modulation is maintained. The second difference is that the kinetic energy caused by the density gradient converges. The third is that the nonlinear regime does not clearly indicate the expansion and collapse of the BEC.

The calculation while maintaining the modulation with  $\gamma = 0.03$  reveals the revival and collapse of the Faraday waves without the nonlinear regime. The energy between the injection and dissipation is balanced, and the kinetic energy oscillates corresponding to the appearance of the Faraday waves. In addition, the revival and collapse of the Faraday waves and the nonlinear regime repeat for the calculation with  $\gamma = 0.01$ . Thus, it is clear that the calculations without  $\gamma$  have different dynamics as compared to those with  $\gamma$ . Because the realistic system encounters certain dissipations, it should behave similar to the system with dissipation described in this paper.

## V. CONCLUSION

We calculated a GP equation to investigate the dynamics of Faraday waves and the nonlinear regime in a cigar-shaped BEC by modulating the interaction. Our calculations were performed for three cases: in the first case, we maintain the modulation; in the second case, the modulation is turned off at  $t_m = 5$  ms without dissi-

TABLE I: Modulation method and results

Modulation method	After applying modulation	After appearance of Faraday waves
Maintaining modulation ( $\gamma = 0$ )	Appearance of Faraday waves	Appearance of nonlinear regime
Turning off modulation ( $\gamma = 0$ )	Same as above	Same as above
Maintaining modulation ( $\gamma = 0.03$ )	Same as above	Revival and collapse of Faraday waves
Maintaining modulation ( $\gamma = 0.01$ )	Same as above	Revival and collapse of Faraday waves and nonlinear regime

pation  $\gamma$ . The third case is maintaining the modulation with  $\gamma$ . When  $\Delta B = 5$  G and  $\omega = 2\omega_r$ , Faraday waves appear in all the calculations. After the appearance of the Faraday waves, the nonlinear regime, which consists of collective modes, appears in the first and second cases. When the nonlinear regime appears in the first case, the BEC expands and shrinks, which is accompanied by dips in the densities intersecting each other, while maintaining their shapes, similar to dark solitons. However, these dips do not represent dark solitons because their profiles are significantly different. Furthermore, for  $\Delta B = 5$  G and  $\omega = 2\omega_r$ , the BEC develops into wave turbulence. In the second case, the expansion and shrink are not observed. Another significant difference between the first and second cases is that the kinetic energy owing to the density gradient increases monotonically in the first case and converges to the static steady state in the second case. It should be noted that the kinetic energies for these two cases accompany quasiperiodic motion.

When  $\gamma = 0.03$ ,  $\Delta B = 5$  G, and  $\omega = 2\omega_r$ , the Faraday patterns continuously appear and collapse without the appearance of the nonlinear regime because the energy between the injection and dissipation is balanced. This dynamics does not reflect the expansion and collapse of the BEC. The kinetic energy owing to the density gradient does not generate quasiperiodic motion, and the energy between the injection and the dissipation is balanced. On the other hand, the calculation with  $\gamma = 0.01$

reflects the appearance of the nonlinear regime after the excitation of the Faraday modes. These excitations appear and collapse repeatedly, and the energy balance occurs at a higher energy than that for  $\gamma = 0.03$ . In summary, our main results are that the revival and collapse of the nonlinear regime require dissipation and the dynamics with and without  $\gamma$  are completely different.

In this study, we investigated the case of modulating the interaction. However, another means of exciting Faraday waves is modulating the trapping potential [19]. If a BEC is modulated by the trapping potential, we expect similar dynamics. Furthermore, another interesting theme is the dynamics of Faraday waves in binary BECs. In this case, the dynamics are investigated by modulating the interaction or the potential. When  $\gamma = 0$ , binary BECs are expected to behave similar to that observed in previous studies [26], and the dynamics may generate the nonlinear regime after the appearance of the Faraday waves. The system with  $\gamma \neq 0$  is realistic but is not studied numerically in the previous works. This study of Faraday waves reflects a good platform for pattern formulation in a BEC.

M.T. acknowledges support from JSPS KAKENHI (Grant Number JP20H01855). We would like to thank Sousuke Inui for helping the analysis used in this work and Editage (www.editage.com) for English language editing.

- 
- [1] P. A. Davidson, *Turbulence: An Introduction for Scientists and Engineers*, 2nd ed. (Oxford University Press, United Kingdom, 2015).
  - [2] D. J. Acheson, *Elementary Fluid Dynamics*, 2nd ed. (Clarendon Press, Clarendon, 1990).
  - [3] G. K. Batchelor, *An Introduction to Fluid Dynamics*, 2nd ed. (Cambridge University Press, Cambridge, 1967).
  - [4] S. Chandrasekhar, *Hydrodynamic and Hydromagnetic Stability*, 1st ed. (Dover Books on Physics, New York, 1981).
  - [5] M. C. Cross and P. C. Hohenberg, *Rev. Mod. Phys.* **65**, 851 (1993).
  - [6] M. Faraday, *Philos. Trans. R. Soc. London* **121**, 299 (1831).
  - [7] T. B. Benjamin and F. Ursell, *Proc. R. Soc. A* **225**, 505 (1954).
  - [8] J. Wu, R. Keolian, and I. Rudnick, *Phys. Rev. Lett* **52**, 1421 (1984).
  - [9] W. S. Edwards and S. Fauve, *Phys. Rev. E* **47**, R788 (1993).
  - [10] W. S. Edwards and S. Fauve, *J. Fluid Mech.* **278**, 123 (1994).
  - [11] A. B. Ezerskii, P. I. Korotin, and M. I. Ravinovich, *JETP Lett.* **41**, 157 (1985).
  - [12] A. B. Ezerskii and M. I. Ravinovich, *Europhys. Lett.* **13**, 243 (1990).
  - [13] N. B. Tuffillaro, R. Ramshankar, and J. P. Gollub, *Phys. Rev. Lett.* **62**, 422 (1989).
  - [14] M. Tubota, M. Kobayashi, and H. Takeuchi, *Physics Reports* **522**, 191 (2013).
  - [15] L. Madeira, A. Cidrim, M. Hemmerling, M. A. Caracanhas, F. E. A. d. Santos, and V. S. Bagnato, *AVS Quantum Science* **522**, 035901 (2020).
  - [16] C. J. Pethick and H. Smith, *Bose-Einstein Condensation in Dilute Gases*, 2nd ed. (Cambridge University Press, Cambridge, 2008).
  - [17] S. Choi, S. A. Morgan, and K. Burnett, *Phys. Rev. A* **57**, 4057 (1998).
  - [18] M. Tsubota, K. Kasamatsu, and M. Ueda, *Phys. Rev. A* **65**, 023603 (2002).

- [19] P. Engels, C. Atherton, and M. A. Hofer, *Phys. Rev. Lett* **98**, 095301 (2007).
- [20] J. H. V. Nguyen, M. C. Tsatsos, D. Luo, A. U. J. Lode, G. D. Telles, V. S. Bagnato, and R. G. Hulet, *Phys. Rev. X* **9**, 011052 (2019).
- [21] K. Staliunas, S. Longhi, and G. J. deValcarcel, *Phys. Rev. Lett* **89**, 210406 (2002).
- [22] A. I. Nicolin, R. Carretero-Gonzalez, and P. G. Kevrekidis, *Phys. Rev. A* **76**, 063609 (2007).
- [23] A. Balaz, R. Paun, A. I. Nicolin, S. Balasubramanian, and R. Ramaswamy, *Phys. Rev. A* **89**, 023609 (2014).
- [24] K. Staliunas, S. Longhi, and G. J. deValcarcel, *Phys. Rev. Lett.* **89**, 210406 (2002).
- [25] K. Staliunas, S. Longhi, and G. J. deValcarcel, *Phys. Rev. A* **70**, 011601(R) (2004).
- [26] A. Balaz and A. I. Nicolin, *Phys. Rev. A* **85**, 023613 (2012).
- [27] Y. Kagan and L. A. Maksimov, *Phys. Rev. A* **64**, 053610 (2001).
- [28] S. Inouye, M. R. Andrews, J. Stenger, H. J. Miesner, D. M. Stamper-Kurn, and W. Ketterle, *Nature* **392**, 151 (1998).
- [29] (), see Supplemental Material 1 at ... for the simulation of the BEC development of the FFT from Faraday waves to the nonlinear regime.
- [30] (), see Supplemental Material 2 at ... for the simulation of the BEC development of the density from Faraday waves to the nonlinear regime.
- [31] N. Navon, A. L. Gaunt, R. P. Smith, and Z. Hadzibabic, *Nature* **539**, 72 (2016).
- [32] N. Navon, C. Eigen, J. Zhang, R. Lopes, A. L. Gaunt, K. Fujimoto, M. Tsubota, R. P. Smith, and Z. Hadzibabic, *Science* **366**, 382 (2019).